Kinetics of the Benzoyl Peroxide/Amine Initiated Free-Radical Polymerization of Dental Dimethacrylate Monomers: Experimental Studies and Mathematical Modeling for TEGDMA and Bis-EM...

ARTICLE *in* MACROMOLECULES · MAY 2004

Impact Factor: 5.8 · DOI: 10.1021/ma049803n

2 AUTHORS:

Dimitris S. Achilias
Aristotle University of Thessaloniki
141 PUBLICATIONS **2,946** CITATIONS
SEE PROFILE

IRINI Sideridou
Aristotle University of Thessaloniki
110 PUBLICATIONS **1,786** CITATIONS
SEE PROFILE

Kinetics of the Benzoyl Peroxide/Amine Initiated Free-Radical Polymerization of Dental Dimethacrylate Monomers: Experimental Studies and Mathematical Modeling for TEGDMA and Bis-EMA

Dimitris S. Achilias and Irini D. Sideridou*

Laboratory of Organic Chemical Technology, Department of Chemistry, Aristotle University of Thessaloniki, GR-541 24, Thessaloniki, Greece

Received January 30, 2004; Revised Manuscript Received March 18, 2004

ABSTRACT: The kinetics of the benzoyl peroxide/amine initiated free-radical cross-linking polymerization of dimethacrylate monomers used as dental materials was studied. The monomers examined were triethylene glycol dimethacrylate (TEGDMA) and ethoxylated bisphenol A glycol dimethacrylate (Bis-EMA). As co-initiator to the benzoyl peroxide (BPO) the new amine 4-(*N*,*N*-dimethylamino)phenethyl alcohol was used. The polymerization rate vs time for several initial initiator concentrations was measured using differential scanning calorimetry. Differences in the polymerization kinetics of the two monomers are discussed in connection with the chemical structure of dimethacrylates Furthermore, a mathematical model was developed to simulate the BPO/amine initiated free-radical polymerization of dimethacrylate monomers. In the elementary reaction mechanism besides initiation, propagation, and termination reactions, also inhibition, primary radical termination, radical trapping, and secondary initiator chain transfer reactions were included. Diffusion-controlled phenomena on the termination, propagation, and initiation reactions were incorporated into the model based on theoretical equations and the free-volume theory. Theoretical simulation results were in good agreement with the experimental data for all different initial initiator concentrations studied.

Introduction

Tertiary aromatic amines have been used for a number of years together with benzoyl peroxide (BPO) as an effective initiation system in the free-radical polymerization of acrylic resins and especially of methyl methacrylate (MMA).[1] The resultant polymers have been widely used as biomaterials in dentistry (denture construction, repair, and relining, temporary crown, and bridge materials) and in orthopedic surgery as bone cements for the stabilization of metallic femoral hip endoprostheses.[2−4] The role of the amine is to carry out the reaction in a short period of time at room (body) temperature. Many amines have been suggested as accelerators, but esthetic and biocompatibility requirements have greatly limited the number of compounds, which can be used for dental or medical applications. The most commonly used amine is *N*,*N* dimethyl-*p*-toluidine (DMT), which is a suspected, but not yet proven, carcinogen[2]. DMT belongs to the *N*-dialkylaminoaromatics, a chemical class structurally alert to DNA reactivity, and also a chromosome-damaging agent inducing numerical chromosome alterations. For this purpose several other amines have been proposed with better biocompatibility than DMT.[5] Among them, 4-(*N*,*N*-dimethylamino)phenethyl alcohol (DMPOH), has been proposed as a more biocompatible[6] and highly reactive accelerator for the polymerization of dental composites.[7] With low amine concentration, nearly colorless restorations having good color stability were obtained. In 1996, DMPOH was been incorporated in a commercial low-viscosity bone cement, Sulfix 60.[8] The kinetics of the BPO/DMPOH redox system compared to BPO/DMT for the polymerization of MMA have been recently studied.[9,10] A point of concern in BPO/amine-initiated polymerizations is whether the maximum rate occurs when equimolar,[9,11] or nonequimolar,[10,12] initial initiator concentrations are used. In our previous publication it was found that when the product of [BPO][amine] was equal to 0.001 M, then the maximum rate occurs when the ratio of [BPO]/[amine] is approximately equal to 1.5.[10] It is worthwhile noting that generally it is undesirable to have an excess of amine remaining in the polymer, because of possible adverse effects on its properties and biocompatibility.

To form highly cross-linked, rigid, and glassy polymer networks with high modulus and solvent resistance, MMA has been replaced by multifunctional monomers such as diacrylates and dimethacrylates. The most widely used resin in dental composites is that based on the copolymer prepared from a combination of 2,2-bis-[*p*-(2′-hydroxy-3′methacryloxypropoxy)phenylene]propane (Bis-GMA) and triethylene glycol dimethacrylate (TEGDMA). TEGDMA is usually added to Bis-GMA in order to achieve workable viscosity limits, since the latter monomer possesses very high viscosity due to the intermolecular hydrogen bonding.[13] However, since these monomers are relatively hydrophilic, there is a growing need to replace them by others more hydrophobic, exhibiting a lower water uptake. The ethoxylated bisphenol A glycol dimethacrylate (Bis-EMA) has been proposed as such a less hydrophilic monomer.[14−16] Bis-EMA has a structure resembling that of Bis-GMA, but without the two hydrophilic −OH groups, which also makes it less viscous. Therefore, in this work the kinetics of the BPO/DMPOH-initiated free-radical polymerization of TEGDMA and Bis-EMA are examined. In this way, results obtained from a dimethacrylate monomer having an aliphatic C−C chain are compared to another dimethacrylate with a stiff central phenyl ring in the C−C chain. The reaction rate profiles and conversion vs time are measured using DSC for different

* To whom correspondence should be addressed. E-mail: siderid@chem.auth.gr.

10.1021/ma049803n CCC: $27.50
Published on Web 05/07/2004

initial initiator concentrations. Initiator combinations were selected such that the reaction would be completed in approximately 10 min since the specifications for dental direct filling resins requires a minimum working time of 1.5 min and a maximum hardening time of 8 min.[17] The amine concentration did not exceed 50 mM (due to material yellowing and biocompatibility reasons).[18]

In this work, a theoretical mathematical model is also developed to simulate the kinetics of the BPO/amine-initiated free-radical polymerization of dimethacrylates. In the elementary reaction, mechanisms besides initiation, propagation, and termination reactions, e.g., inhibition, primary radical termination, radical trapping, and secondary initiator chain transfer reactions are included. Diffusion-controlled phenomena on the termination, propagation, and initiator reactions are incorporated into the model based on the theoretical equations proposed by Achilias and Kiparisides[19] and the free-volume theory.

The most prominent feature of free-radical cross-linking polymerization reactions involving multifunctional monomers is the strong influence of diffusional effects arising due to the formation of an infinite network. Several researchers have developed mathematical models for the photopolymerization kinetics of multimethacrylate and multiacrylate monomers.[20−40] Andrzejewska[41] has recently reviewed most of these. In the kinetic mechanism of the cross-linking polymerization, besides the conventional elementary reactions, the effect of primary radical termination,[30,31] radical trapping,[36] and inhibition[42] have been examined. Furthermore, diffusion phenomena play an important role, especially in the termination reaction. In cross-linking polymerization, termination is diffusion-controlled immediately from the beginning of the reaction due to a rapid increase in system viscosity. Macroradicals and polymer chains become entangled or cross-linked in the network, leading thus to a suppression of the center of mass diffusion of macroradicals used by them in order to find one another and react. However, radicals can still implicitly move in space and approach each other through reaction with unreacted double bonds (reaction diffusion). As the polymerization proceeds and the glass transition of the mixture becomes greater than the polymerization temperature, vitrification effects begin to limit the mobility of even small molecules such as the monomer or primary initiator radicals. Under these conditions, the rate of the propagation and the initiation reactions also significantly drop.

According to our knowledge, there is not any detailed model taking into account all the above phenomena (kinetic and diffusional) for the simulation of the free-radical cross-linking polymerization of dimethacrylate monomers using the BPO/amine initiation system.

Experimental Section

Materials. The dimethacrylate monomers used in this work included triethylene glycol dimethacrylate (TEGDMA) (Aldrich Chem. Co., Lot No. 461111, inhibited) and ethoxylated bisphenol A glycol dimethacrylate (Bis-EMA) (Aldrich Chem. Co., Lot No. 03514HF, inhibited with 500 ppm monomethyl ether hydroquinone), and they were used as received without further purification. Figure 1 shows the chemical structure for each of these monomers. The initiators used were DMPOH (mp = 59−61 °C) (from Aldrich) used without further purification and BPO (from Fluka) purified by fractional recrystallization from ethanol (mp = 104 °C). All other chemicals used were reagent grade.

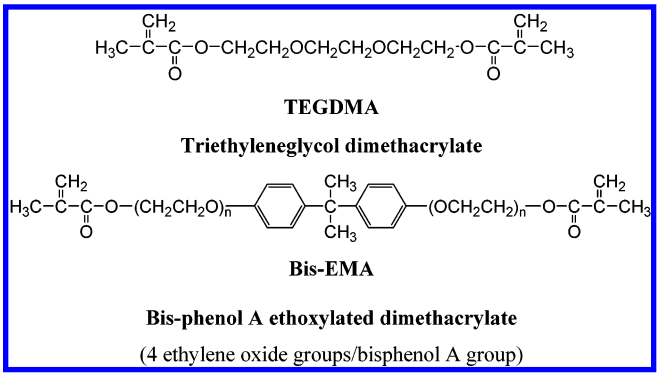

Figure 1. Chemical structures of the dimethacrylate monomers studied.

Procedure. Two initial stock solutions in each dimethacrylate monomer were prepared, one containing BPO (0.02 *m*) and the other DMPOH (0.05 *m*). After successive dilution with the monomer, all other initial initiator concentrations until 0.01 *m* (molality) were obtained. The initial monomer mixture with the two initiators was prepared by mixing equal amounts (approximately 0.5 g) from the two separate initiator solutions.

The polymerization kinetics of the various formulations was studied using differential scanning calorimetry (DSC). Experiments were performed in a nitrogen atmosphere using the DSC-Pyris 1 (Perkin-Elmer) equipped with the Pyris software for windows. Indium was used for the enthalpy and temperature calibration of the instrument. In each experiment a standard mass from the monomer mixture (15−20 mg) was placed in an aluminum Perkin-Elmer sample pan, weighted, and placed into the appropriate position of the instrument. To minimize loss of monomer due to evaporation, all samples were sealed. All polymerizations were carried out at 37 °C and the reaction temperature was continuously recorded and maintained constant (within ±0.01 °C) during the whole conversion range. The reaction exotherm (in normalized values, W/g) at a constant temperature was recorded as a function of time. The rate of heat release (d(Δ*H*)/d*t*) measured by the DSC was directly converted into the overall reaction rate (d*x*/d*t*) using the following formula

$$\frac{dx}{dt} = \frac{1}{\Delta H_T}\frac{d(\Delta H)}{dt} \qquad (1)$$

where ΔH_T denotes the total reaction enthalpy calculated from the product of the number of double bonds per monomer molecule ($n = 2$) times the standard heat of polymerization of a methacrylate double bond ($\Delta H_0 = 54.9$ kJ/mol)[36] over the monomer molecular weight, i.e., $\Delta H_T = n\Delta H_0/MW_m$.

The degree of conversion was calculated by integrating the area between the DSC thermograms and the baseline established by extrapolation from the trace produced after complete polymerization (no change in the heat produced during the reaction). All the experimental results reported in the Results and Discussion are taken from an average of at least two experiments.

Model Development

Kinetic Mechanism. Tertiary aromatic amines accelerate the free-radical decomposition of BPO, by a complex mechanism, which involves first a S_N2 nucleophilic displacement leading to an intermediate adduct and finally to the formation of a benzoyloxy radical, benzoic acid and a *N*-methylene radical, according to the reaction presented in Figure 2.[1,43,44] The formation of *N*-methylene radical was confirmed by electron spin resonance (ESR),[45] and the presence of the above-mentioned radical was detected by UV analysis in the polymer formed, indicating the efficiency of this radical in the initiation process of polymerization.[44]

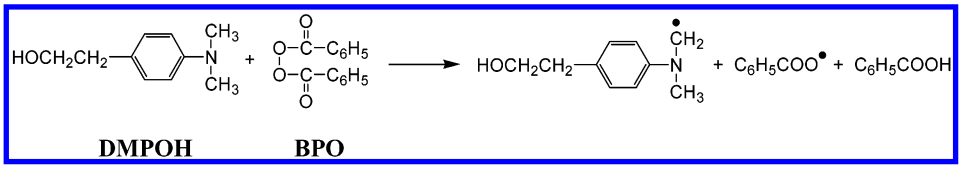

Figure 2. Formation of the primary initiator radicals from the reaction of BPO with DMPOH.

If the symbols A and I are used to denote the amine and the peroxide initiator molecules respectively, then the following general reaction mechanism for the free-radical polymerization of multifunctional monomers can be written:

initiation: $A + I \xrightarrow{k_d} I^\bullet + A^\bullet +$ inert products (2)

$$I^\bullet + M \xrightarrow{k_{i1}} P_1^\bullet \quad (3)$$

$$A^\bullet + M \xrightarrow{k_{i2}} P_1^\bullet \quad (4)$$

propagation: $P_n^\bullet + M \xrightarrow{k_p} P_{n+1}^\bullet$ (5)

termination by combination/disproportionation:

$$P_n^\bullet + P_m^\bullet \xrightarrow{k_t} D_{n+m}/D_n + D_m \quad (6)$$

radical trapping: $P_n^\bullet \xrightarrow{k_b} P_{n,b}^\bullet$ (7)

primary radical termination: $I^\bullet + P_n^\bullet \xrightarrow{k_{tp}} D_n$

$$A^\bullet + P_n^\bullet \xrightarrow{k_{tp}} D_n \quad (8)$$

chain transfer to amine: $P_n^\bullet + A \xrightarrow{k_{fA}} D_n + A^\bullet$ (9)

inhibition: $P_n^\bullet + Z \xrightarrow{k_z} D_n$ (10)

benzoyl peroxide side reaction:

$$I^\bullet + I \xrightarrow{k_I} I^\bullet + \text{inert products} \quad (11)$$

In the above kinetic scheme, the symbols $I^\bullet$ and $A^\bullet$ are used to denote radicals formed by the fragmentation of the benzoyl peroxide and the amine, respectively, M is a monomer unit, Z is the inhibitor, $P_n^\bullet$ and $P_{n,b}^\bullet$ are used to identify the respective "live" macroradicals which are active or trapped and containing n monomer units and finally, D_n stands for the "dead" polymer formed containing n monomer units.

According to this reaction mechanism, during the initiation step two different primary radicals are formed, which in this work are assumed to be both capable of reacting with a monomeric double bond and initiate polymerization. Two populations of "live" macroradicals are assumed: those which are "active" and take part in the propagation and the termination reactions and those which are "trapped" in the polymer main network and thus do not react. Radical trapping is assumed to take place by a unimolecular first-order reaction. Because radical trapping is presumed to be permanent, it affects the rate in a manner similar to unimolecular termination.[36] Besides the trapping, "live" radicals terminate also by three different mechanisms (eqs 8, 9, and 10). The bimolecular termination reaction is lumped into a single reaction with rate constant k_t.[31] The primary radical termination (eq 8) is quite often in commercial polymerization reactions, where high initial initiator concentrations are used in order to achieve fully cured products in short reaction times.[30] Finally, chain transfer to amine (eq 9) is considered as the third chain termination reaction mechanism, since it is generally known that tertiary amines act as chain-transfer agents in the polymerization of methacrylates, by the standard hydrogen abstraction mechanism.[46,47] Furthermore, the monomers used contain an amount of inhibitor to prevent premature reactions. Oxygen also trapped in the sample pans can act as an inhibitor in the free-radical polymerization of methacrylates. It is therefore important to include the inhibition reaction (eq 10) in the kinetic mechanism for a more complete description of the possible elementary reactions taking place during polymerization. The reinitiation process of inhibited chains is considered negligible. Finally, it was found[10,48] that BPO may react with its own primary radicals or primary radicals formed from the decomposition of the amine to form also another primary radical $C_6H_5COO^*$

Table 1. Detailed Material Balances

initiators

$$\frac{1}{V}\frac{d(V[I])}{dt} = -k_d[I][A] - k_I[I^\bullet][I]$$

$$\frac{1}{V}\frac{d(V[A])}{dt} = -k_d[I][A] - k_{fA}[P^\bullet][A]$$

primary initiator radicals

$$\frac{1}{V}\frac{d(V[I^\bullet])}{dt} = f_1 k_d[I][A] - k_{i1}[I^\bullet][M] - k_{tp}[I^\bullet][P^\bullet]$$

$$\frac{1}{V}\frac{d(V[A^\bullet])}{dt} = f_2 k_d[I][A] - k_{i2}[A^\bullet][M] - k_{tp}[A^\bullet][P^\bullet] + k_{fA}[P^\bullet][A]$$

double bonds

$$\frac{1}{V}\frac{d(V[M])}{dt} = -k_p[P^\bullet][M] - (k_{i1}[I^\bullet] + k_{i2}[A^\bullet])[M] \quad \text{or}$$

$$\frac{dx}{dt} = k_p[P^\bullet](1 - x)$$

active "live" macroradicals

$$\frac{1}{V}\frac{d(V[P^\bullet])}{dt} = k_{i1}[M][I^\bullet] + k_{i2}[M][A^\bullet] - 2k_t[P^\bullet]^2 - k_Z[Z][P^\bullet] - k_b[P^\bullet] - k_{fA}[A][P^\bullet] - k_{tp}([I^\bullet] + [A^\bullet])[P^\bullet]$$

trapped "live" macroradicals

$$\frac{1}{V}\frac{d(V[P^\bullet]_b)}{dt} = k_b[P^\bullet]$$

inhibitor

$$\frac{1}{V}\frac{d(V[Z])}{dt} = -k_Z[Z][P^\bullet]$$

where

$$[P^\bullet] = \sum_{n=1}^{\infty} P_n^\bullet$$

and other inactive products. This reaction has been included as eq 11 in the kinetic mechanism.

Material Balances. On the basis of the general kinetic mechanism presented in eqs 2−11 for the free-radical polymerization of multifunctional monomers, detailed material balances for all the reacting species can be written. These appear in Table 1. In this table, molar balances are included for the two initiators (peroxide and amine) used, the concentration of the double bonds, the primary initiator (BPO and amine) radicals, the active and trapped "live" macroradicals, and finally the inhibitor. In this work, the two commonly used assumptions of the quasi-steady-state approximation (QSSA) for the macroradicals and the primary radicals are not employed. Furthermore, the long-chain hypothesis (LCH) can be used for the calculation of the double bond conversion. The system of eight coupled ordinary differential equations appeared in Table 1 are numerically integrated to give the time dependence of all reacting species. Gear's method is used, which is suitable for solving stiff sets of differential equations. The change in all the kinetic rate constants during the reaction is considered according to the diffusion equations presented in the next section.

Diffusion-Controlled Reactions

Termination and Propagation. Several models have been proposed in the literature in order to quantify the effect of diffusion on the mobility of reacting species in a polymerizing system. In this study, the theoretical equations developed by Achilias and Kiparissides,[19] considering also the correction proposed by Zhu et al.[49] and Litvinencko and Kaminsky,[50] were used. Accordingly, the final expressions for the termination and the propagation rate constants are written as

$$\frac{1}{k_t} = \frac{1}{k_{t_0}} + \frac{1}{4\pi N_A r_t D_p} \tag{12}$$

$$\frac{1}{k_p} = \frac{1}{k_{p_0}} + \frac{1}{4\pi N_A r_p D_m} \tag{13}$$

where k_{t0} and k_{p0} are the true kinetic rate constants for termination and propagation, respectively, r_t and r_p represent the effective reaction radii for termination and propagation, and finally, D_p and D_m denote the polymer and monomer diffusion coefficients, respectively.

Furthermore, the primary radical concentration rate constant, k_{tp}, was considered to be diffusion-controlled in the same manner as k_p; therefore, an equation similar to eq 12 was employed. This assumption is correct since the diffusion-controlled characteristics of primary radical termination and propagation both depend on the diffusion of a small molecule (i.e., primary radical or monomer) in order to find a "live" macroradical and react.

Initiation. Taking into account the effect of diffusion-controlled phenomena on the initiation reaction, a mathematical model had been developed previously.[19] Following this model, the final expression for the initiator efficiency is expressed as

$$\frac{f_0}{f} = 1 + \frac{C}{D_I} \tag{14}$$

where f_0 is used to denote the initial initiator efficiency factor, D_I is the diffusion coefficient of primary radicals, and C is a lumped constant including geometrical features of the cage in which the primary initiator radicals are trapped and the initial initiation reaction rate constant.

In eq 14, the effect of possible loss of primary radicals through the recombination reactions is considered in f_0. When D_I is very large (i.e., at initial monomer conversions) then f is equal to f_0, however when the mobility of the primary radicals is hindered as the polymerization precedes, the diffusion coefficient, D_I is decreased leading to decreased initiation efficiency. In this investigation it was assumed that the two efficiency factors of the initiating reactions, i.e., those from primary radicals formed from the decomposition of BPO and the amine, f_1 and f_2, respectively, were equal ($f_1 = f_2 = f$). However, this assumption needs further examination.

Radical Trapping. The radical trapping rate constant, k_b, is assumed to depend on the fractional free volume of the mixture V_f according to[36]

$$k_b = k_{b0}\frac{1}{e^{-\gamma_b/V_f}} \tag{15}$$

where k_{b0} is the preexponential factor and γ_b is the dimensionless activation volume which governs the rate at which radical trapping increases as a function of fractional free volume.[36]

Calculation of Reaction Radius. For the calculation of the radius of interaction for termination, r_t, the so-called flexible-chain limit was adopted.[51,52] According to this approach, a polymer chain is characterized by nodes of entanglement every j_c monomer units (it is these nodes that restrict the center of mass motion of the chain as a whole), and then r_t will be given by the distance of the chain end from the node of entanglement closest to it, i.e., $r_t^2 = j_c\alpha^2$, where j_c is the entanglement spacing and α is the root-mean-square end-to-end distance per square root of the number of monomer units. The radius of interaction of the propagation reaction, r_p, can be approximated by half the Lennard-Jones diameter, σ, of the monomer,[51,52] $r_p = \sigma/2$.

Calculation of Diffusion Coefficients. In this study, all the diffusion coefficients were calculated using the free-volume theory, which has been proven to be adequate in describing diffusion-controlled phenomena in free-radical polymerization.[53−55] Several diffusion models based on the free volume theory have been proposed in the literature.[56] Among them the model of Fujita[57] has been employed in this work since it requires a minimum number of parameters.[56,58] Accordingly, the diffusion coefficients of the small molecules (monomer, D_m, and primary initiator radicals, D_I) are expressed as:[56,57]

$$D_m = D_{m0}\exp\left(-\frac{\gamma_m}{V_f}\right) \tag{16}$$

$$D_I = D_{I0}\exp\left(-\frac{\gamma_I}{V_f}\right) \tag{17}$$

where D_{m0} and D_{I0} are the preexponential factors depending only on temperature and γ_m and γ_I are the corresponding overlapping factors, depending only on the size of the diffusing molecule and not on the temperature or on the polymer concentration. The fractional free volume, V_f, is calculated in the subsequent section.

To derive an equation for the polymer diffusion coefficient D_p, two different physical phenomena should be considered. The first is associated with the reduced mobility of the center of mass of a reacting macroradical, $D_{p,d}$, which can be simulated using the free volume theory, while the second is related to the so-called termination by reaction−diffusion, $D_{p,rd}$. D_p can then be calculated as

$$D_p = D_{p,d} + D_{p,rd} \tag{18}$$

the diffusion coefficient $D_{p,d}$ is calculated according to the free volume theory, using an equation similar to eqs 16 and 17, as

$$D_{p,d} = \frac{D_{p0}}{\bar{M}_w^{\,n}} \exp\left(-\frac{\gamma_t}{V_f}\right) \tag{19}$$

where D_{p0} is a preexponential factor depending only on temperature and γ_t, the overlapping factor depending on the size of the diffusion molecule. The exponent n in eq 19 had been set equal to 2 according to the reptation theory.[19] However, in cross-linked systems, the polymer diffusion coefficient is not considered to depend on the molecular weight;[20,25,30] thus the value of $n = 0$ was adopted in this investigation

According to the reaction−diffusion termination mechanism, when the polymer network is formed, radicals suspended in the backbone polymer network are physically separated in space and they are unable to terminate. However, eventually these radicals may move in a close proximity and react by propagating through monomeric or pendant double bonds. Thus, the propagation reaction is a means for physical movement of the radical. This termination mechanism has been proven by several authors to be the dominant mechanism even in highly cross-linked methacrylate systems.[25,52,59−60] Accordingly, the diffusion coefficient $D_{p,rd}$ should be proportional to the frequency of monomer addition to the radical chain:[25,51,52]

$$D_{p,rd} = \frac{2}{3}\alpha^2 k_p[M] \tag{20}$$

Fractional Free Volume. The fractional free volume is the sum of the equilibrium fractional free volume, $V_{f,\infty}$ and the excess fractional free volume, $V_{f,e}$:[20,25] $V_f = V_{f,\infty} + V_{f,e}$. The equilibrium fractional free volume of the mixture is expressed as

$$V_{f,\infty} = V_{fm}(1 - \varphi_p) + V_{fp}\varphi_p \tag{21}$$

with

$$V_{fm} = 0.025 + \alpha_m(T - T_{gm}); \qquad V_{fp} = 0.025 + \alpha_p(T - T_{gp}) \tag{22}$$

and

$$\varphi_p = \frac{x(1 - \epsilon_\nu)}{1 - x\epsilon_\nu} \tag{23}$$

Here, the subscripts m and p refer to monomer and polymer, respectively, φ_p is the volume fraction of polymer, T is the reaction temperature, T_g is the glass transition temperature, α is the volume expansion coefficient and ϵ_ν is the volume contraction factor determined by $\epsilon_\nu = (\nu_m - \nu_p)/\nu_m$ where ν is the specific volume of every component.

Table 2. Induction Time, Maximum Polymerization Rate, Time at the Maximum Polymerization Rate, and Maximum Double Bond Conversion for the Polymerization of TEGDMA at 37 °C

BPO (m)	DMPOH (m)	induction time (min)	R_p^{max} ($\times 10^3$ s^{-1})	time (min) at R_p^{max}	X_{max} (%)
0.02	0.05	0	6.5	1.4	65
0.02	0.02	0.6	4.7	2.9	60
0.02	0.015	1.3	4.1	4.1	61
0.02	0.01	2.3	3.7	5.6	64
0.015	0.05	0.1	6.1	1.7	64
0.015	0.02	1.5	4.1	4.1	60
0.015	0.015	2.2	3.3	5.4	62
0.015	0.01	3.8	2.9	7.8	59
0.01	0.05	0.7	5.6	2.8	64
0.01	0.02	2.1	3.3	5.3	59
0.01	0.015	3	2.8	7.7	57
0.01	0.01	4.9	2.4	9.4	60

The excess fractional free volume, $V_{f,e}$ is added in the fractional free volume of the system in order to take into account volume relaxation effects.[20,25] According to these authors, $V_{f,e}$ is calculated using the equilibrium specific volume, ν_∞, from:

$$V_{f,e} = \frac{(\nu - \nu_\infty)}{\nu_\infty} \tag{24}$$

ν_∞ is determined as a function of conversion, x, the volume contraction factor, ϵ_ν, and the monomer specific volume, ν_m, according to ν_∞.

The rate of change of the specific volume, ν, is considered proportional to the deviation from the equilibrium specific volume and the proportionality constant is characteristic of the system and inversely related to the relaxation time, τ, so that[20,25]

$$\frac{d\nu}{dt} = \frac{-(\nu - \nu_\infty)}{\tau} \tag{25}$$

Finally, the free-volume dependence of the relaxation time, τ, is calculated from $\tau = C_1 + C_2/V_f$.

Results and Discussion

Results on the BPO/DMPOH-Initiated Polymerization of TEGDMA. The induction time, the maximum polymerization rate, R_p^{max}, the time to achieve R_p^{max}, and the maximum double bond conversion of all the experiments carried out under different initial initiator concentrations appear in Table 2. As the initial initiator concentration is lowered, the induction time is increased, meaning that at low initial initiator values the primary radicals formed were scavenged by dissolved oxygen. The maximum polymerization rate values are increased following increased initial initiator concentrations. It is noteworthy, however, that the maximum double bond conversion, X_{max}, is roughly the same in all initial initiator concentrations, showing only a slightly increased value at the higher initial initiator concentrations. The average value for X_{max} was 61%, which means that the average number of double bonds reacted per monomer is approximately 1.2.

Furthermore, simulation results from the mathematical model are compared to experimental data during the full reaction rate vs time period. All the kinetic rate constants and the physical parameters used to model the BPO/DMPOH-initiated polymerization of TEGDMA

Table 3. Kinetic Rate Constants and Physical Properties for the BPO/DMPOH-Initiated Polymerization of TEGDMA

parameter	ref	parameter	ref
$k_d = 3.5 \times 10^{-3}$ L/(mol s)	10	$\gamma_m = 0.7$	this study
$f_0 = 1$	48	$\gamma_b = 0.7$	36
$k_{p0} = 1500$ L/(mol s)	66	$\gamma_I = 0.41$	36
$k_{t0} = 3.5 \times 10^6$ L/(mol s)	this study	$\gamma_t = 2$	this study
$k_{i1} = k_{i2} = k_{p0}$	31	$\alpha_m = 0.0005$ K^{-1}	24, 36
$k_{tp0} = 1.0 \times 10^8$ L/(mol s)	30	$\alpha_p = 0.000075$ K^{-1}	24, 36
$k_{b0} = 1 \times 10^{-10}$ 1/s	this study	$T_{gm} = -83.4$°C	62
$k_Z = 4.5 \times 10^7$ L/(mol s)	31	$T_{gp} = 300$°C	33
$k_I = 5 \times 10^6$ L/(mol s)	this study	$\alpha = 0.69$ nm	19, 52
$k_{fA}/k_p = 0.1$	47	$\sigma = 0.79$ nm	19, 52
$\rho_m = 1.092$ g/mL	Aldrich	$j_c = 13$	this study
$\rho_p = 1.239$ g/mL	61	$D_{m0} = 5 \times 10^{-6}$ cm^2/s	this study
$\epsilon_v = 0.119$	calcd	$D_{p0} = 40$ cm^2/s	this study
$[M]_0 = 7.636$ mol/L	calcd	$C/D_{I0} = 3 \times 10^{-4}$	this study

are listed in Table 3. Although the developed model requires a large number of parameters, most can be determined independently of the reaction considered. The initiator decomposition rate constant, k_d, had been calculated for this initiator system in ref 10. For the chain transfer to DMPOH rate constant, k_{fA}, a value reported for chain transfer of a methacrylate radical to *N*,*N*-dimethylaminoethyl methacrylate (i.e., $k_{fA}/k_p = 0.1$) was adopted.[47] The effect of this value on polymerization reaction rate was subsequently examined. The initial concentration $[M]_0$ was calculated on the basis of a monomer molecular weight of 286. For the relaxation parameters, the values proposed in ref 19 (i.e., $C_1 = -0.5$ and $C_2 = 0.01$) were used. The monomer glass transition temperature was set equal to −83.4 °C,[62] which is very close to a value reported recently (−85 °C) in the literature.[63] The polymer glass transition temperature was taken from the literature.[33] It should be noted here that it is very difficult to measure the T_g value of 100% polymer. Lu et al.[64] reported a T_g value of "completely cured" TEGDMA as 135 °C. However, there is a misconception in the phrase of "completely cured TEGDMA". Allen et al.[65] also measured a value of T_g for poly(TEGDMA) as 135 °C. However, they reported that although the polymer was postcured at 150 °C until it showed no residual exotherm during DSC tests, it could not be driven to full cure. Using a separate technique (proton enhanced/magic angle spinning NMR), they[65] estimated the ultimate degree of TEGDMA curing to be 88%. Thus, they concluded that this must be the ultimate state of cure even though residual unsaturation was determined. This was attributed to the fact that the oligo(ethylene glycol) links are too short to give the networks sufficient flexibility for all vinyl groups to react. Therefore, we think that the theoretical value reported in ref 33, which was estimated from extrapolation to 100% conversion using experimental data at different conversion levels and the free volume theory, reflects better the polymer glass transition temperature.

Furthermore, the two principal parameters k_{p0} and k_{t0}, governing mainly the polymerization rate, have to be evaluated. To calculate the best possible values for these parameters, the experimentally measured initial reaction rate, R_{p0}, was used. The procedure that we followed for the calculation of R_{p0} is briefly discussed next. The polymerization rate that was measured experimentally at a given initial initiator concentration was plotted vs double bond conversion. After approximately 0.6% conversion and until approximately 3−4% conversion a straight line was observed in all conditions. The slope of this line was determined and extrapolated to zero double bond conversion, as shown in Figure 3.

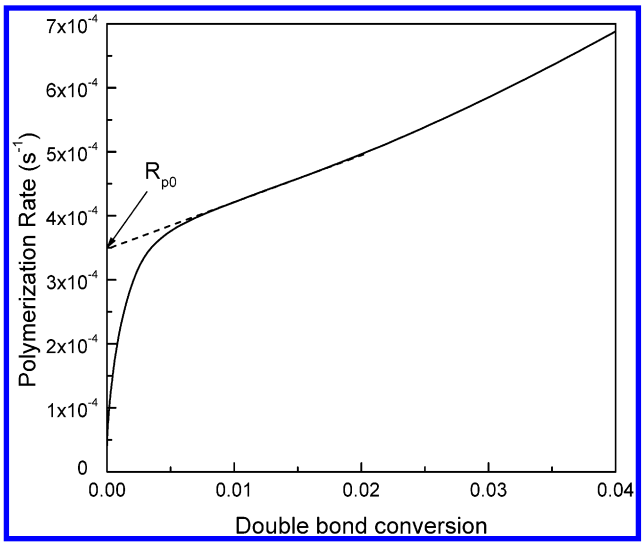

Figure 3. Calculation of the initial polymerization rate R_{p0}.

Thus, the initial polymerization rate estimated refers to zero double bond conversion. It should be noted here that from a physical point of view R_p at zero double bond conversion should be zero (as it is shown also in Figure 3). However, since the free-radical polymerization rate reaches a steady-state value after a short time period we used these R_{p0} values in order to calculate the initial propagation and termination rate constants. Theoretically, if R_{p0} is calculated using the QSSA, just after the inhibition period, assuming that the contribution of the trapping radical and the primary radical termination reaction is negligible, then the following equation is obtained:

$$R_{p0} = \frac{k_{p0}}{(2k_{t0})^{1/2}}((f_1 + f_2)k_d)^{1/2}([I]_0[A]_0)^{1/2} \qquad (26)$$

Initially, all the kinetic rate constants are constant. Hence, by plotting the experimentally measured initial polymerization rate as a function of the product $([I]_0[A]_0)^{1/2}$ for different initial initiator concentrations, a straight line should arise with a slope of $k_{p0}[(f_1 + f_2)k_d/(2k_{t0})]^{1/2}$. As can be shown from Figure 4, all the assumptions made are correct leading to a very good straight line ($R = 0.999$) with an intercept of -8×10^{-7} and a slope of 0.033 L/(mol s). If we keep the value obtained for $(f_1 + f_2)k_d$ in our laboratorly,[10] then the following value is obtained for $k_{p0}/(2k_{t0})^{1/2} = 0.56$ (L/(mol s))$^{1/2}$. Lovell et al.[66] had calculated experimentally k_{p0} and k_{t0} values for the photopolymerization of TEGDMA. If we use the value for k_{p0} that they proposed, i.e., 1500 L/

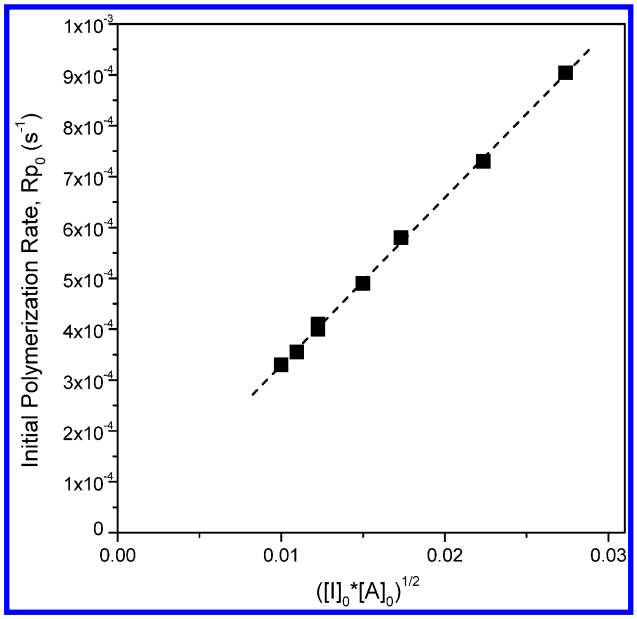

Figure 4. Calculation of the true initial kinetic rate constants k_{p0} and k_{t0} using the initial polymerization rate vs the product $([I_0][A_0])^{1/2}$ at several initial initiator concentrations.

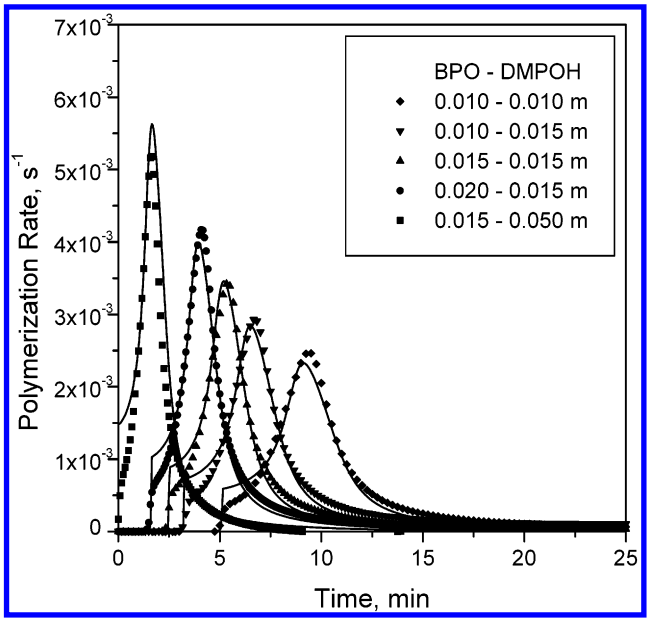

Figure 5. Comparison of the experimental and simulated polymerization rate vs time curves for TEGDMA polymerization at 37°C and at several initial initiator concentrations.

(mol s), then we calculate a value for k_{t0} of 3.5×10^6 L/(mol s) which is very close to the value that the above authors had also proposed. Hence, these values for the true propagation and termination rate constants were used.

Finally, the overlapping γ factor (γ_t and γ_m), as well as the preexponential factors, D_{p0}, D_{m0}, D_{I0}, and j_c were estimated in this study. The values of these parameters were obtained by fitting the simulation model results on polymerization rate and conversion, to the experimental data at initial concentrations of BPO and DMPOH equal to 0.015 *m*.

Having evaluated all the parameters, the differential equations listed in Table 1, together with eq 25 were numerically integrated using also the algebraic equations for the diffusion-controlled phenomena (eqs 12−24). Figure 5 shows the predicted polymerization rate vs time, compared with the experimental data of the polymerization of TEGDMA at 37 °C obtained under different initial initiator concentrations. As it can be seen the parameters obtained using the initial equimolar concentration of 0.015 *m* without any modification, can equally well predict the experimental data for a variety of equal or unequal initial initiator concentrations. The value and location of the maximum rate of polymerization are both reproduced to within a few percent with just a slight underestimation of the experimental data at the initial reaction times. As can be seen from Figure 5, as the initial initiator concentration is increased, the inhibition time is shortened and greater values for the maximum rate constant are observed (see also Table 2). By integration of the reaction rate, the double bond conversion with respect to time can be obtained, which is plotted in Figure 6. Again simulation results and experimental data are in good agreement.

The effect of diffusion-controlled phenomena on the polymerization rate is explained next, using the curves showing the variation of the termination and propagation rate constants, as well as the initiator efficiency during the reaction (Figure 7). The dashed lines are used to distinguish between the different kinetic regions

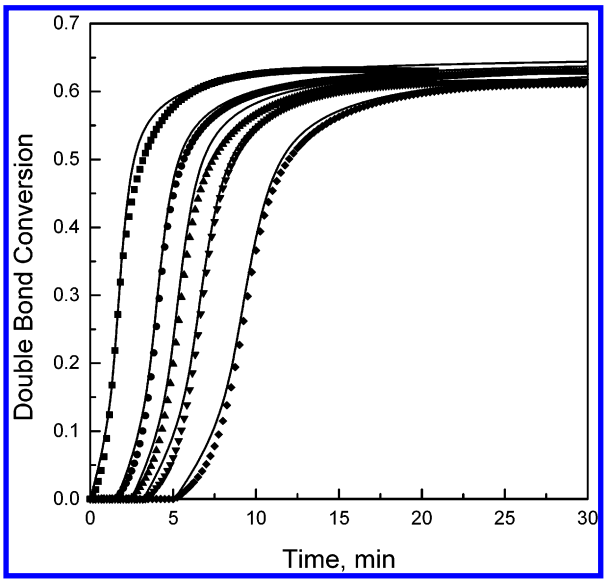

Figure 6. Comparison of the fractional double bond conversion vs time simulation results to the experimental data measured by DSC during the polymerization of TEGDMA at 37°C (initial initiator concentrations as in Figure 4).

encountered in the polymerization. The fact that autoacceleration takes place almost from the beginning of the reaction is obvious from this figure, since k_t retains a constant value only for a very short conversion period. During this period polymerization rate is almost constant together with the active radical concentration shown in Figure 8. In the conversion range 0.5−26%, the termination of active radicals is diffusion-controlled, since it involves the simultaneous diffusion and subsequently reaction of two macroradicals, which are hindered to move. The termination rate constant falls continuously, while k_p and f remain almost constant. A decrease in k_t brings about an increase in the active radical concentration, while the "trapped" radical concentration is still low (Figure 8). Consequently, the primary initiator-amine radicals, A*, formed from the chain transfer reaction (eq 9) are also increased. At a

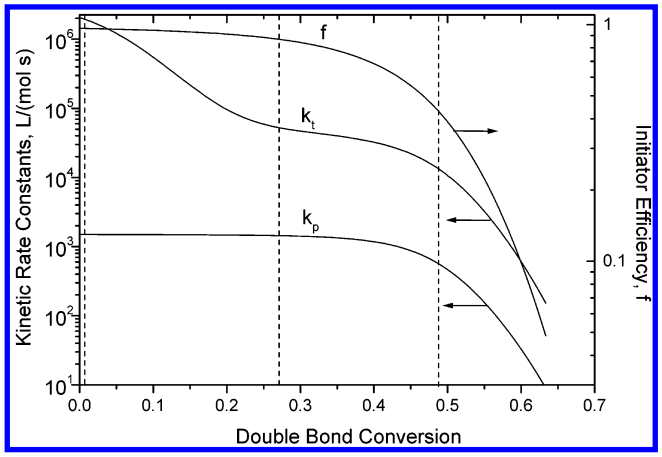

Figure 7. Termination (k_t) and propagation (k_p) rate constants, as well as initiator efficiency (f) vs double bond conversion for the BPO/DMPOH initiated polymerization of TEGDMA. Initial initiator concentrations $[BPO]_0 = [DMPOH]_0 = 0.015$ *m*.

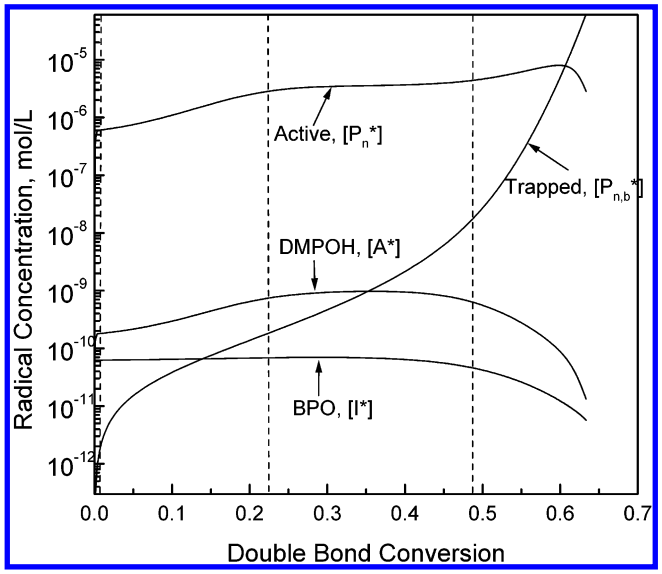

Figure 8. Active and trapped radical concentrations together with primary BPO and DMPOH radical concentrations vs double bond conversion for the polymerization of TEGDMA (conditions same as in Figure 6).

certain point (around 26% conversion) a plateau in the variation of k_t appears that depicts the contribution of the reaction−diffusion-controlled termination. At this point termination occurs only by the implicit movement of radicals through the propagation reaction. This transition is obvious in the reaction rate profiles as the maximum appearing in every curve. In this region the drop of the termination rate constant slows down while k_p is still constant. This leads to a very slow increase of the active radical concentration, while the initiator efficiency starts to drop due to the decrease of the primary radical diffusion coefficient. As a result, the number of initiator primary radicals, which are able to initiate new polymer chains, falls. At this stage, the polymerization rate significantly drops. This is due to the continuous reduction of double bonds through the propagation reaction, while termination is almost constant. In summary, at this stage, two physical phenomena take place simultaneously: the initiator efficiency starts to drop and the termination rate constant becomes reaction−diffusion-controlled. It should be noticed here that the approximate 26% conversion where the maximum in the reaction rate appears in Figure 5, is close to the 23% corresponding value observed in the literature concerning the photopolymerization of DEGDMA.[36] To include the reaction−diffusion term in their model Bowman and co-workers[24,27,30,31] have used the expression $k_t = Rk_p[M]$. If we use the parameter values obtained in this approach for the polymerization of TEGDMA, the corresponding value for R obtained is approximately equal to 6. This value is very close to the value of $R = 5$ that was experimentally observed by Lovell et al.[66] for the photopolymerization of TEGDMA.

As the polymerization proceeds, at double bond conversion values around 50%, the mobility of monomer molecules is hindered, and thus the propagation reaction starts to fall, leading also to a second decrease in the termination reaction, which is already governed by the propagational movement. During this stage, the initiator efficiency also significantly falls and thus the concentration of both primary initiator radicals decreases. At this final stage, the radical trapping becomes severe as the active radical concentration starts to drop. This radical trapping and the diffusion-controlled propagation cause the polymerization rate to decrease much more rapidly than the rate, which can be accounted for by the depletion of functional groups. At a certain point, the systems glass transition temperature reaches the reaction temperature and polymerization ceases.

Following this, the two elementary reactions included for the first time in this study, concerning the chain transfer to amine (eq 9) and the side reaction of BPO (eq 11), are examined in relation to their effect on polymerization rate and radical concentrations. The effects of the chain transfer to amine rate constant, k_{fA}, on the polymerization rate, active radical concentration, and primary initiator-amine-radical concentration is shown in Figure 9. As the chain transfer to amine reaction is more pronounced (greater values for k_{fA}) the active radical population is lowered due to their reaction with the amine molecules. This also leads to lower polymerization rate values, while the primary radicals formed, A*, are increased. Also if k_{fA} is set equal to zero the primary amine radicals, A*, follow the same trend with the primary BPO radicals; i.e., they are constant until the time where the initiator efficiency drops where they also decrease. If this chain transfer reaction occurs to a great extent (approximately $5k_p$ in this study), a great decrease in the A* concentration is observed after a constant value period. This is attributed to a great consumption of the amine molecules and thus a loss of one initiator before the end of the reaction, leading also to less final conversion values.

Furthermore, the effects of the initiator side reaction denoted with k_I, on the polymerization rate, active radical concentration and primary initiator-BPO-radical concentration is shown in Figure 10. As this initiator side reaction is more pronounced (greater values for k_I), lowered polymerization rate values are obtained as a result of also lowered active radical population concentrations. The primary initiator-BPO radicals exhibit also lowered values. Since explicitly the I* concentration is not influenced by this side reaction it is the reduction in the initial initiator (BPO) molecules caused by the greater extent of their reaction with the I* radicals, that gives rise to the above observations. If this reaction occurs to a great extent (approximately $k_I = 10^8$ L (mol s) in this study) a great decrease in the initiator (BPO) molecules is observed with a corresponding decrease in

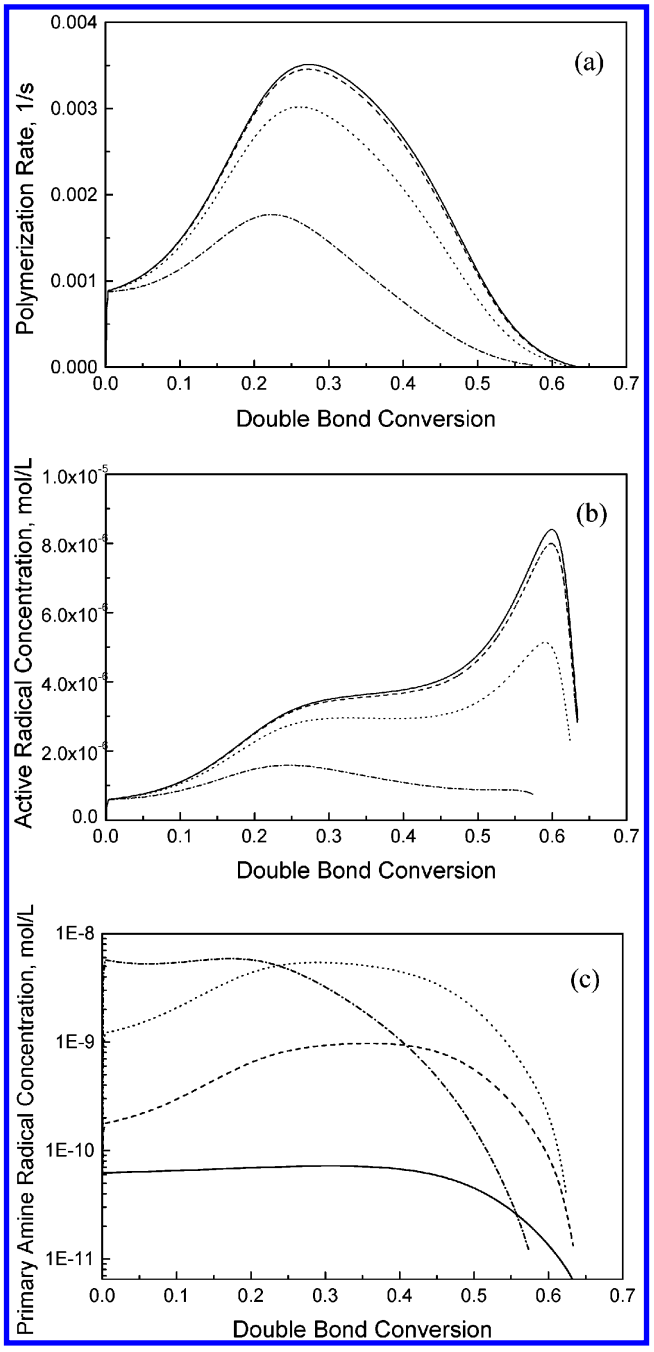

Figure 9. Effects of the chain transfer to amine rate constant, k_{fA}, on the polymerization rate (a), active radical concentration (b), and primary DMPOH radical concentration (c) vs double bond conversion for the polymerization of TEGDMA at experimental conditions same as in Figure 6. Straight line: $k_{fA} = 0$. Dashed line: $k_{fA} = 0.1\ k_p$. Dotted line: $k_{fA} = 1\ k_p$. Dash−dotted line: $k_{fA} = 5\ k_p$.

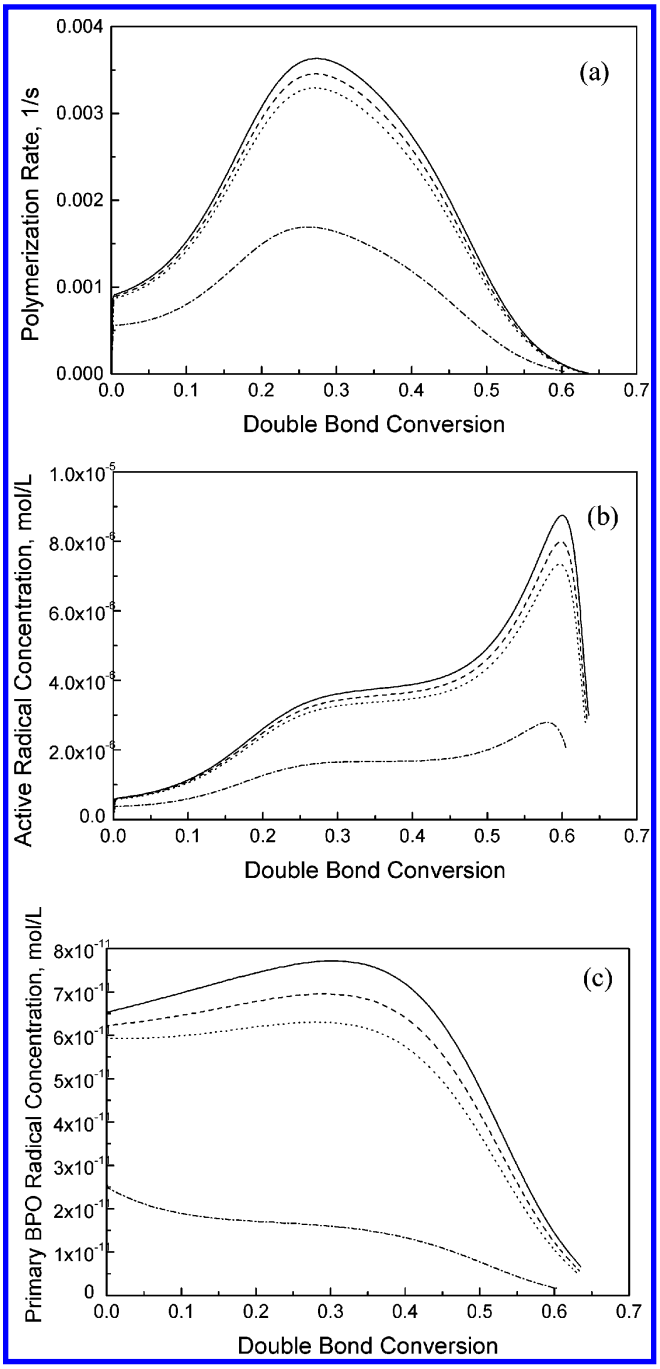

Figure 10. Effects of the initiator side reaction rate constant, k_I, on the polymerization rate (a), active radical concentration (b), and primary BPO radical concentration (c) vs double bond conversion, for the polymerization of TEGDMA at experimental conditions same as in Figure 6. Straight line: $k_I = 0$. Dashed line: $k_I = 5 \times 10^6$ L/(mol s). Dotted line: $k_I = 10 \times 10^6$ L/(mol s). Dash−dotted line: $k_I = 100 \times 10^6$ L/(mol s).

I* concentration, leading to very low active radical concentration and thus polymerization rate.

Results on the BPO/DMPOH-Initiated Polymerization of Bis-EMA. Bis-EMA has a much greater molecular size (540) compared to TEGDMA (286) and therefore lower initial concentration of double bonds, so the latter at equal degrees of conversion will exhibit a higher density of cross-linking and will form tighter networks. The induction time, the maximum polymerization rate, R_p^{max}, the time to achieve R_p^{max} and the maximum double bond conversion of all the experiments carried out under different initial initiator concentrations appear in Table 4. According to the comments made in the case of the TEGDMA polymerization, an increase in the initial initiator concentration leads to a decrease in the induction time and of the time to achieve the maximum polymerization rate, while the maximum polymerization rate values are increased. The corresponding values of the induction time and the time to achieve R_p^{max}, obtained in Bis-EMA polymerization are in general greater than those measured in TEGDMA. Furthermore, the maximum polymerization rate and the maximum double bond conversion always presented lower corresponding values. The average value of X_{max} was 46%, which was also lower than the corresponding

Table 4. Induction Time, Maximum Polymerization Rate, Time at the Maximum Polymerization Rate, and Maximum Double Bond Conversion for the Polymerization of Bis-EMA at 37 °C

BPO (*m*)	DMPOH (*m*)	induction time (min)	R_p^{max} ($\times 10^3$ s^{-1})	time (min) at R_p^{max}	X_{max} (%)
0.02	0.05	0.0	2.1	1.9	50
0.02	0.02	1.5	0.9	7.0	49
0.02	0.015	3.8	0.5	9.6	46
0.02	0.01	6.1	0.3	14.0	45
0.015	0.05	0.0	1.6	2.1	48
0.015	0.02	4.9	0.5	11.0	45
0.015	0.015	7.4	0.2	15.5	45
0.015	0.01	12.0	0.1	23.5	44
0.01	0.05	0.0	1.3	2.6	48
0.01	0.02	8.3	0.2	16.0	47
0.01	0.015	9.1	0.2	18.3	45
0.01	0.01	12.5	0.1	26.9	48

in the case of TEGDMA. In this case, the average number of double bonds reacted per monomer is approximately 0.92. These observations could be attributed macroscopically to the greater viscosity of the Bis-EMA monomer (approximately 3 Pa s)[63] compared to the TEGDMA (0.05 Pa s).[63] As it is well-known, the viscosity is a measure of the resistance of molecules to flow and a high viscosity value is indicative of the presence of intermolecular interactions. These interactions can cause a decreased mobility of monomer molecules during polymerization (lower polymerization rate) as well as a decreased flexibility of the corresponding polymeric network. From a microscopic point of view the lower maximum double bond conversion observed in Bis-EMA polymerization compared to TEGDMA can be well explained using the monomer glass transition temperatures. Bis-EMA, due to the presence of the rigid aromatic nuclei, exhibits higher T_g (−46 °C)[62] than TEGDMA (−83.4 °C).[62] This higher monomer T_g brings about a higher T_g of the polymerizing system. As is well-known, the reaction ceases as the glass transition temperature of the reacting system approaches the polymerization temperature. Thus, it is the greater T_g of the mixture that causes the polymerization to stop earlier at lower degrees of double bond conversion.

In Figure 11, the polymerization rate vs conversion observed from the polymerization of Bis-EMA is compared to the corresponding values of the TEGDMA reaction under two different initial initiator concentrations. As it can be seen always the reaction rate values obtained using TEGDMA are greater than those of Bis-EMA. Also the final double bond conversion from TEGDMA was higher than that of Bis-EMA, meaning that the aliphatic chain of TEGDMA can more easily move in space and thus reacts to a greater extent. The same trend has been also observed and explained in the photopolymerization of these two monomers.[62]

Furthermore, to compare the experimental data on the BPO/DMPOH-initiated polymerization of Bis-EMA to the simulation model results the model parameters have to be evaluated. The kinetic rate constants and the physical properties, which have been used in this system, are listed in Table 5. The parameters related to the initiators (k_d, f_0) and inhibitor (k_Z) were kept the same as in the TEGDMA polymerization. Also the same values were used for the primary radical termination (k_{tp}), initiator side reaction (k_I), and chain transfer to amine (k_{fA}) rate constants, as well as for γ_m. The initial concentration $[M]_0$ was calculated on the basis of a monomer molecular weight of 540. The monomer glass

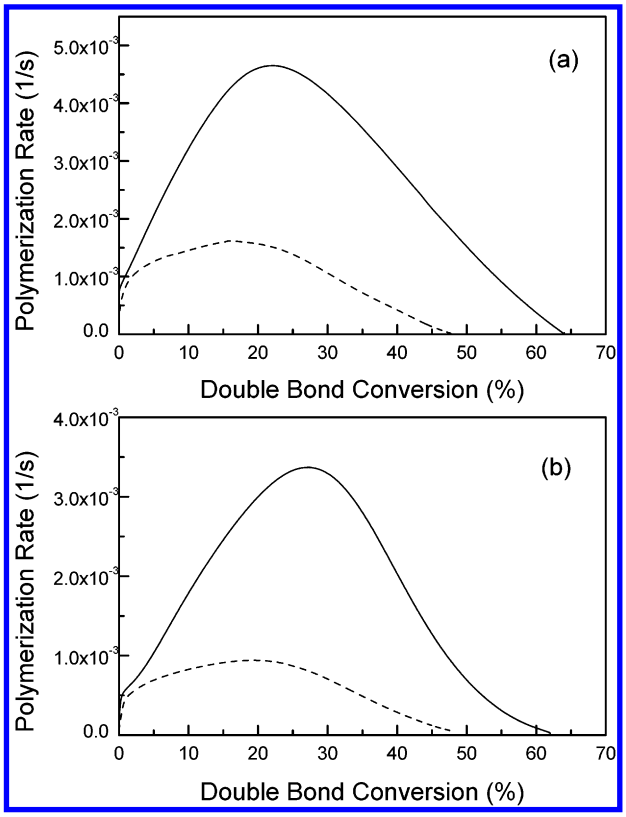

Figure 11. Comparison of the polymerization rates vs double bond conversion between TEGDMA (straight line) and Bis-EMA (dashed line) at initial initiator concentrations of BPO−DMPOH: 0.015−0.05 (a) and 0.015−0.015 *m* (b).

transition temperature was set equal to −46 °C,[62] which is close to a value reported recently (−42 °C) in the literature.[63] For the polymer glass transition temperature, the same value with TEGDMA was used since there was not anything else available in the literature. Furthermore, k_{p0} and k_{t0} were estimated in a similar way to that reported in TEGDMA polymerization. By plotting again the experimentally measured initial polymerization rate as a function of the product $([I]_0[A]_0)^{1/2}$ for different initial initiator concentrations, a straight line arose, providing thus the ratio $k_{p0}/(k_{t0})^{1/2} = 0.22$ (L/(mol s))$^{1/2}$. In the photopolymerization of the same monomer, Cook[21] reported a value of 0.2 (L/(mol s))$^{1/2}$ for this ratio. However, still there exists the problem of estimating the individual parameters for k_{p0} and k_{t0}. Since we were not able to provide additional experimental data and no corresponding values were found in the literature, we assumed a value of 10^6 L/(mol s) for k_{t0} and calculated $k_{p0} = 220$ L/(mol s). This assumption was made in order for k_{t0} to be of the same order of magnitude as the corresponding value reported for TEGDMA. However, this assumption needs further examination.

Finally, the preexponential factors, D_{p0}, D_{m0}, and D_{I0} together with γ_t and j_c were calculated in this study. The values of these parameters were obtained by fitting the simulation model results on polymerization rate and conversion, to the experimental data at initial concentrations of BPO and DMPOH equal to 0.02 *m*.

Having evaluated all the parameters, the differential equations listed in Table 1, together with eq 25 were numerically integrated using also the algebraic equations for the diffusion-controlled phenomena (eqs 12−24). Figure 12 shows the predicted polymerization rate

Table 5. Kinetic Rate Constants and Physical Properties for the BPO/DMPOH Initiated Polymerization of Bis-EMA

parameter	ref	parameter	ref
$k_{p0} = 220$ L/(mol s)	this study	$\gamma_t = 1.7$	this study
$k_{t0} = 1 \times 10^6$ L/(mol s)	this study	$\gamma_m = 0.7$	this study
$k_{b0} = 1 \times 10^{-9}$ 1/s	this study	$\gamma_b = 0.7$	36
$k_{tp0} = 1.0 \times 10^8$ L/(mol s)	30	$\gamma_I = 0.41$	36
$k_I = 5 \times 10^6$ L/(mol s)	this study	$T_{gm} = -46$°C	62
$k_{fA}/k_p = 0.1$	47	$T_{gp} = 300$ °C	33
$\rho_m = 1.120$ g/mL	Aldrich	$j_c = 365$	this study
$\rho_p = 1.197$ g/mL	61	$D_{m0} = 25 \times 10^{-6}$ cm^2/s	this study
$\epsilon_v = 0.064$	calcd	$D_{p0} = 3.8$ cm^2/s	this study
$[M]_0 = 4.15$ mol/L	calcd	$C/D_{I0} = 5 \times 10^{-4}$	this study

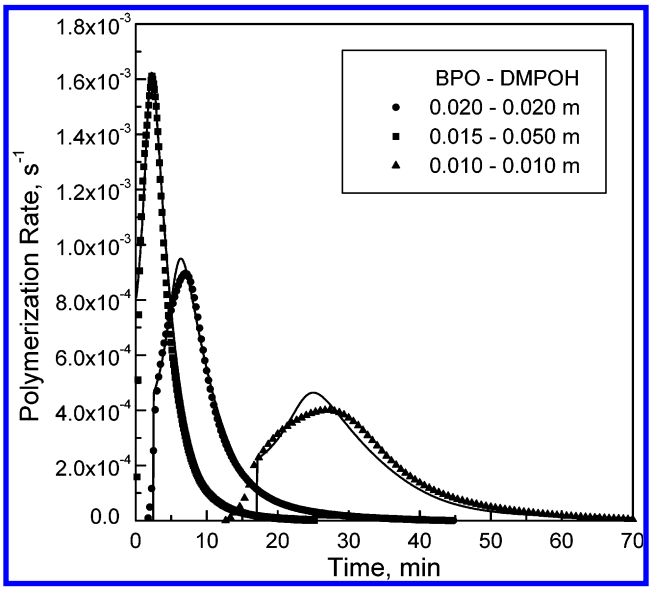

Figure 12. Comparison of the experimental and simulated polymerization rate vs time curves for Bis-EMA polymerization at 37°C and at different initial initiator concentrations.

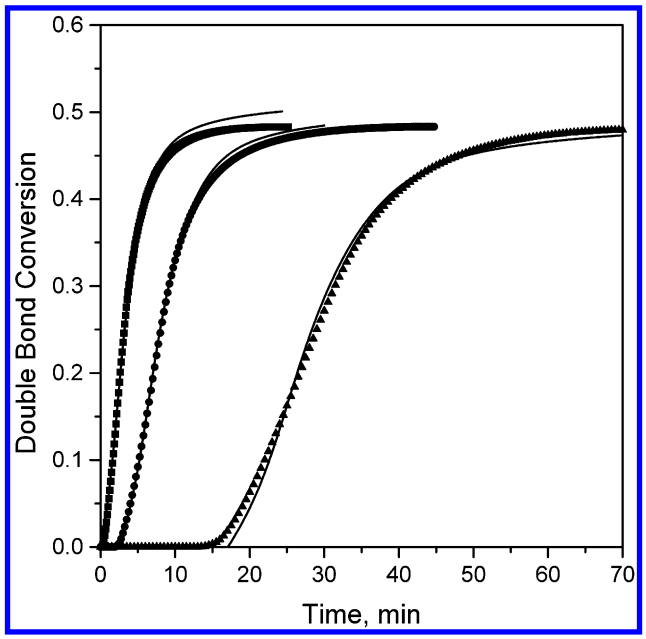

Figure 13. Comparison of the experimental data and simulation results on the fractional conversion vs time for Bis-EMA polymerization at 37°C (initial initiator concentrations as in Figure 12).

vs time, compared with the experimental data of polymerization of Bis-EMA at 37 °C obtained under different initial initiator concentrations. As it can be seen the parameters obtained in initial concentration of 0.02 *m* without any modification can equally well

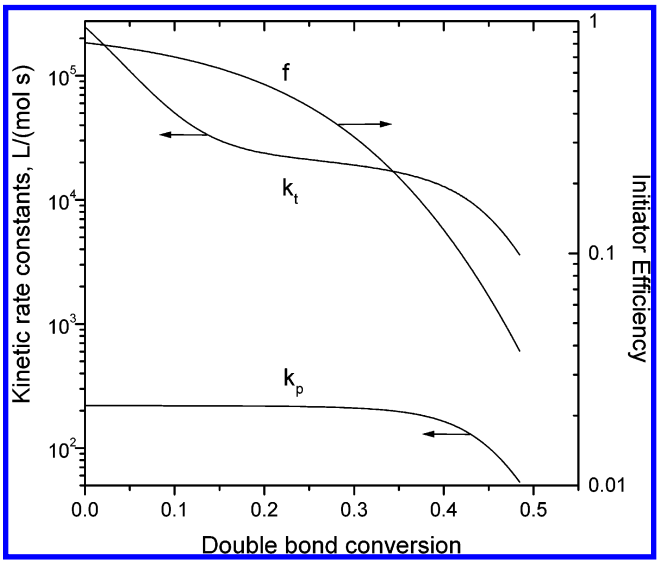

Figure 14. Termination (k_t) and propagation (k_p) rate constants, as well as initiator efficiency (f) vs double bond conversion for the BPO/DMPOH initiated polymerization of Bis-EMA. Initial initiator concentrations $[BPO]_0 = [DMPOH]_0 = 0.02$ *m*.

predict the experimental data for a variety of equal or unequal initial initiator concentrations. The variation of the double bond conversion with respect time is shown in Figure 13. Again simulation results and experimental data are in very good agreement. On comparing the polymerization rate curves obtained for Bis-EMA with the corresponding for TEGDMA some critical differences are visible which can be explained in a k_t, k_p, and f vs conversion plot (Figure 14). First of all the lower polymerization rate is explained with lower initial values in the propagation rate constant together with the termination rate constant. Second the plateau observed in the variation of k_t (i.e., control of the termination by the reaction−diffusion mechanism) covers a much more broad conversion region (from approximately 16% to 42%). This means that very early the center of mass of radicals cannot easily diffuse in space and termination occurs only through the addition of monomeric double bonds to the active radicals. Finally, the initiator efficiency, *f*, falls much more abruptly and sooner during the reaction.

Conclusions

In this investigation, the kinetics of the benzoyl peroxide/amine-initiated free-radical cross-linking polymerization of TEGDMA and Bis-EMA used as dental materials were studied. The polymerization rate vs time for several initial initiator concentrations was measured using DSC. To simulate the polymerization reaction a mathematical model was developed based on a detail

elementary reaction mechanism (included initiation, propagation, and termination reactions, as well as primary radical termination, inhibition, radical trapping, and secondary initiator chain transfer reactions). Diffusion-controlled phenomena in the termination, propagation, and initiation reactions were incorporated into the model based on theoretical equations and the free-volume theory. Theoretical simulation results were in good agreement to the experimental data for all different initial initiator concentrations. Finally, it seems that TEGDMA having an aliphatic C−C chain results in higher maximum double bond conversions and polymerization rates compared to Bis-EMA, which is more viscous and includes aromatic rings in the C−C chain.

References and Notes

(1) Moad, G.; Solomon, D. H. *The Chemistry of Free Radical Polymerization; Pergamon Press*: Oxford, U.K., 1995; pp 72−73.
(2) Williams, D., Ed. *Concise Encyclopedia of Medical & Dental Materials;* Pergamon Press: Oxford, U.K., 1990; pp 8−21.
(3) Craig, R. G. Prosthetic Applications of Polymers. In *Restorative Dental Materials*, 10th ed.; Mosby-Year Book Inc.: St. Louis, MO, 1997; pp 500−514.
(4) Linden, L. A. Dental Polymers. In *Polymeric Materials Encyclopedia*, Salamone, C. J., Ed.; CRC Press Inc.: New York, 1996; Vol. 3 D−E, p 1839.
(5) Vazquez, B.; Levenfeld, B.; San Roman, J. *Polym. Int.* **1998**, *46*, 241−250.
(6) Miller, E. G.; Washington, U. H.; Zimmerman, E. R.; Bowles, W. H. *J. Dent. Res.* **1984**, *63*, 312−316.
(7) Brauer, G. M.; Stansbury, J. W.; Antonucci, J. M. *J. Dent. Res.* **1981**, *60*, 1343−1348.
(8) Fritsch, E. W. *J. Biomed. Mater. Res.* **1996**, *31*, 451−456.
(9) Oldfield, F. F.; Yasuda, H. K. *J. Biomed. Mater. Res.* **1999**, *44*, 436−445.
(10) Achilias, D. S.; Sideridou, I. *J. Macromol. Sci., Part A: Pure Appl. Chem.* **2002**, *A39*, 1435−1450.
(11) Vazquez, B.; Deb, S.; Bonfield, W. *J. Mater. Sci., Mater. Med.* **1997**, *7*, 455−460.
(12) Bowen, R. L.; Argentar, H. A. *J. Appl. Polym. Sci.* **1973**, *17*, 2213−2222.
(13) Sankarapandian, M.; Shobha, H. K.; Kalachandra, S.; McGrath, J. E.; Taylor, D. F. *J. Mater. Sci.: Mater. Med.* **1997**, *8*, 465−468.
(14) Moszner, N.; Ulrich, S. *Prog. Polym. Sci.* **2001**, *26*, 535−576.
(15) Sideridou, I.; Tserki, V.; Papanastasiou, G. *Biomaterials* **2003**, *24*, 655−665.
(16) Sideridou, I.; Achilias, D. S.; Spyroudi, C.; Karabela, M. *Biomaterials* **2004**, *25*, 367−376.
(17) Council on Dental Materials and Devices, New American Dental Association Specification No. 27 for Direct Filling Resins. *JADA 94* **1977**, 1191−1194.
(18) Dulik, D. M. *J. Dent. Res.* **1979**, *58*, 1308−1316.
(19) Achilias, D. S.; Kiparissides, C. *Macromolecules* **1992**, *25*, 3739−3750.
(20) Bowman, C. N.; Peppas, N. A. *Macromolecules* **1991**, *24*, 1914−1920.
(21) Cook, W. D. *Polymer* **1992**, *33*, 2152−2161.
(22) Cook, W. D. *Polymer* **1992**, *33*, 600−609.
(23) Cook, W. D. *J. Polym. Sci., Part A: Polym. Chem.* **1993**, *31*, 1053−1067.
(24) Anseth, K. S.; Bowman, C. N. *Polym. React. Eng.* **1993**, *1*, 499−520.
(25) Kurdikar, D. L.; Peppas, N. A. *Macromolecules* **1994**, *27*, 4084−4092.
(26) Kurdikar, D. L.; Peppas, N. A. *Macromolecules* **1994**, *27*, 733−738.
(27) Goodner, M. D.; Lee, H. R.; Bowman, C. N. *Ind. Eng. Chem. Res.* **1997**, *36*, 1247−1252.
(28) Scott, R. A.; Peppas, N. A. *Macromolecules* **1999**, *32*, 6149−6158.
(29) Lecamp, L.; Youssef, B.; Bunel, C.; Lebaudy, P. *Polymer* **1999**, *40*, 1403−1409.
(30) Goodner, M. D.; Bowman, C. N. *Macromolecules* **1999**, *32*, 6552−6559.
(31) Goodner, M. D.; Bowman, C. N. *Chem. Eng. Sci.* **2002**, *57*, 887−900.
(32) Elliott, J. E.; Bowman, C. N. *Macromolecules* **1999**, *32*, 8621−8628.
(33) Elliott, J. E.; Lovell, L. G.; Bowman, C. N. *Dent. Mater.* **2001**, *17*, 221−229.
(34) Elliott, J. E.; Anseth, J. W.; Bowman, C. N. *Chem. Eng. Sci.* **2001**, *56*, 3173−3184.
(35) Elliott, J. E.; Bowman, C. N. *Macromolecules* **2002**, *35*, 7125−7131.
(36) Wen, M.; McCormick, A. V. *Macromolecules* **2000**, *33*, 9247−9254.
(37) Berchtold, K. A.; Lovestead, T. M.; Bowman, C. N. *Macromolecules* **2002**, *35*, 7968−7975.
(38) Bogacki, M. B.; Andrzejewska, E.; Andrzejewski, M. *Polimery* **2001**, *46*, 721−724.
(39) Bogacki, M. B.; Andrzejewska, E.; Andrzejewski, M. *Polimery* **2002**, *47*, 734−737.
(40) Andrzejewska, E.; Bogacki, M. B.; Andrzejewski, M. *Macromol. Theory Simul.* **2001**, *10*, 842−849.
(41) Andrzejewska, E. *Prog. Polym. Sci.* **2001**, *26*, 605−665.
(42) Batch, G. L.; Macosko, C. W. *J. Appl. Polym. Sci.* **1992**, *44*, 1711−1729.
(43) Pryor, W. A.; Hendrickson, W. H. Jr. *Tetrahedron Lett.* **1983**, *24*, 1459−1462.
(44) De Feng, X. *Makromol. Chem., Macromol. Symp.* **1992**, *63*, 1−18.
(45) Sato, T.; Kita, S.; Otsu, T. *Makromol. Chem.* **1975**, *176*, 561−571.
(46) Hoyle, C.; Keel, M.; Kim, K.-J. *Polymer* **1988**, *29*, 18−23.
(47) Seretoudi, G.; Sideridou, I. *J. Macrom. Sci. Pure Appl. Chem.* **1995**, *A32*, 1183−1195.
(48) Stickler, M.; Dumont, E. *Makromol. Chem.* **1986**, *187*, 2663−2673.
(49) Zhu, S.; Tian, Y.; Hamielec, A. E.; Eaton, D. R. *Macromolecules* **1990**, *23*, 1144−1150.
(50) Litvinenko, G. I.; Kaminsky, V. A. *Prog. React. Kinet.* **1994**, *19*, 139−193.
(51) Russell, G. T.; Napper, D. H.; Gilbert, R. G. *Macromolecules* **1988**, *21*, 2133−2140.
(52) Young, J. S.; Bowman, C. N. *Macromolecules* **1999**, *32*, 6073−6081.
(53) O'Neil, G. A.; Wisnudel, M. B.; Torkelson, J. M.*Macromolecules* **1996**, *29*, 7477−7490.
(54) O'Neil, G. A.; Wisnudel, M. B.; Torkelson, J. M. *Macromolecules* **1998**, *31*, 4537−4545.
(55) O'Neil, G. A.; Torkelson, J. M.*Macromolecules* **1999**, *32*, 411−422.
(56) Masaro, L.; Zhu, X. X. *Prog. Polym. Sci.* **1999**, *24*, 731−775.
(57) Fujita, H. *Adv. Polym. Sci.* **1961**, *3*, 1.
(58) Zetterlund, P. B.; Johnson, A. F. *Polymer* **2002**, *43*, 2039−2048.
(59) Anseth, K. S.; Kline, L. M.; Walker, T. A.; Anderson, K. J.; Bowman, C. N. *Macromolecules* **1995**, *28*, 2491−99.
(60) Mateo, J. L.; Serrano, J.; Bosch, P. *Macromolecules* **1997**, *30*, 1285−88.
(61) Kalachandra, S.; Turner, D. T. *J. Biomed. Mater. Res.* **1987**, *21*, 329−338.
(62) Sideridou, I.; Tserki, V.; Papanastasiou, G. *Biomaterials* **2002**, *23*, 1819−29.
(63) Dickens, S. H.; Stansbury, J. W.; Choi, K. M.; Floyd, C. J. E. *Macromolecules* **2003**, *36*, 6043−53.
(64) Lu, H.; Lovell, L. G.; Bowman, C. N. *Macromolecules* **2001**, *34*, 8021−25.
(65) Allen, P. E. M.; Simon, G. P.; Williams, D. R. G.; Williams, E. H. *Macromolecules* **1989**, *22*, 809−16.
(66) Lovell, L. G.; Stansbury, J. W.; Syrpes, D. C.; Bowman, C. N. *Macromolecules* **1999**, *32*, 3913−21.

MA049803N